Supplementary Information (SI) for Energy & Environmental Science.

Electronic Supplementary Information for

Ligand Engineering of Solution-Processed NiO_x for High-Performance n-i-p Perovskite Photovoltaics

Fang Cao,† Xinfeng Dai,† Di Tian,† Yingchen Peng, Jun Yin, Jing Li,* Ye Yang, Nanfeng Zheng,* and Binghui Wu**

Correspondence to: caofang@xmu.edu.cn, lijing@xmu.edu.cn, nfzheng@xmu.edu.cn, binghuiwu@xmu.edu.cn

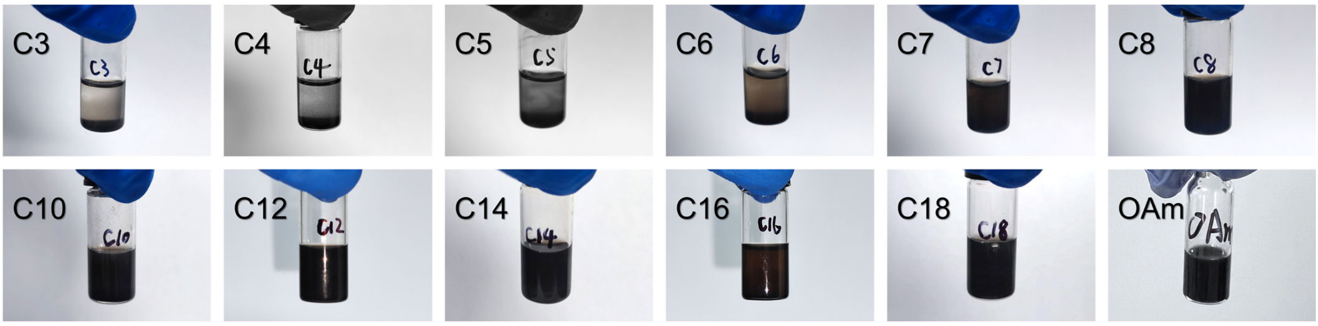

Figure S1. Photos of varied alkylamine-modulated NiO_x inks.

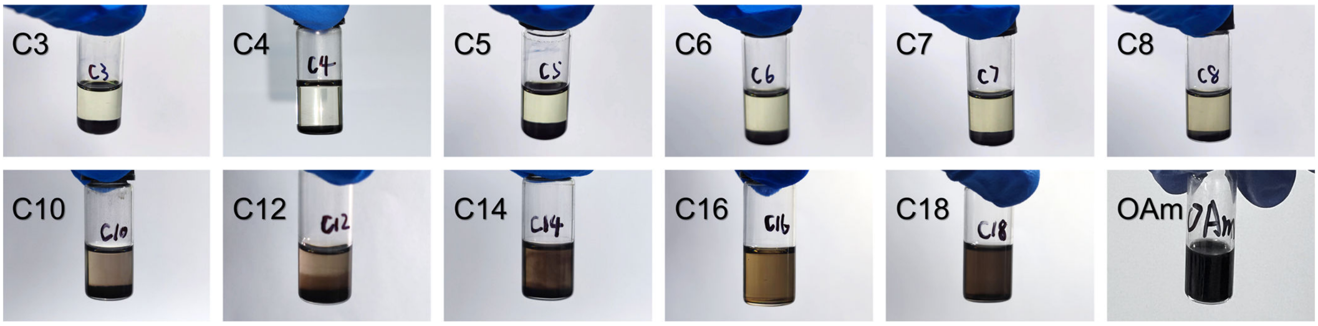

Figure S2. Photos of varied alkylamine-modulated NiO_x inks after aging for 4 hours.

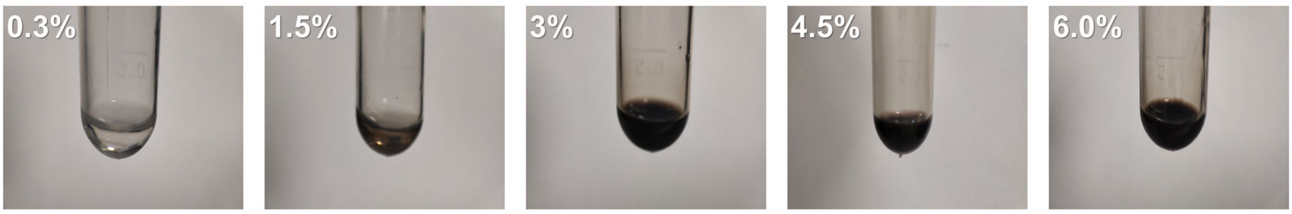

Figure S3. Photographs of NiO_x inks modulated by OAm at different molar ratios.

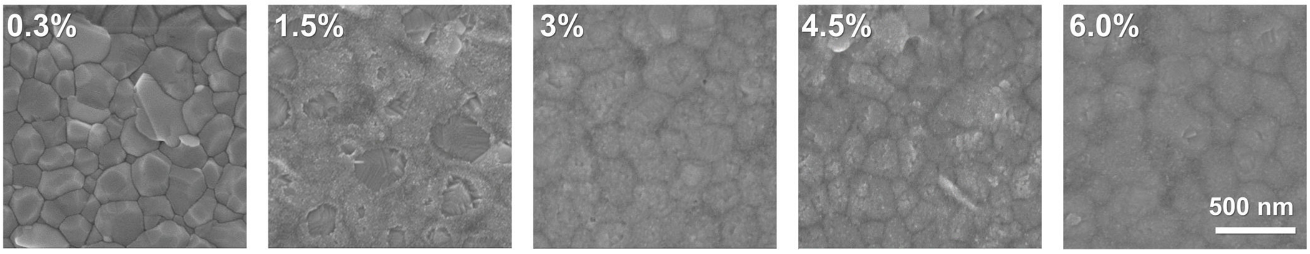

Figure S4. SEM images of NiO_x films modulated by OAm at different molar ratios.

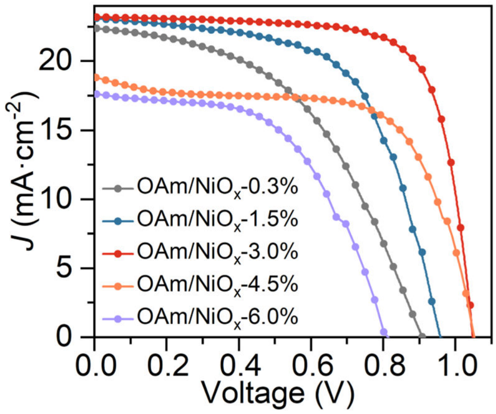

Figure S5. Optimal *J*−*V* curves of PSCs with NiO_x HTLs modulated by OAm at different molar ratios.

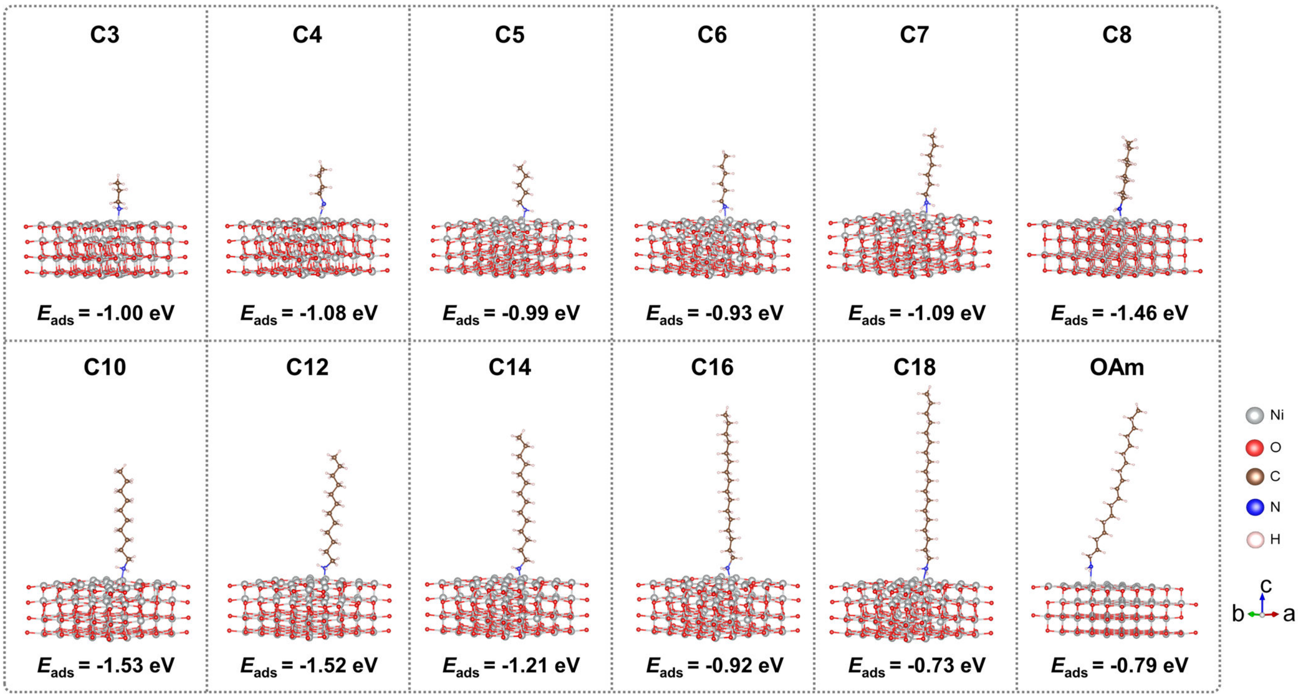

Figure S6. Adsorption configurations of varied amines on NiO(100).

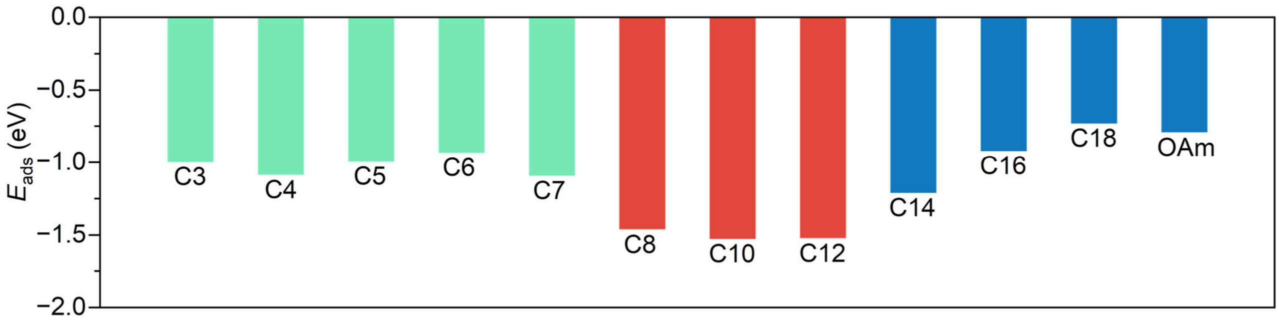

Figure S7. Adsorption energies of varied amines on NiO(100).

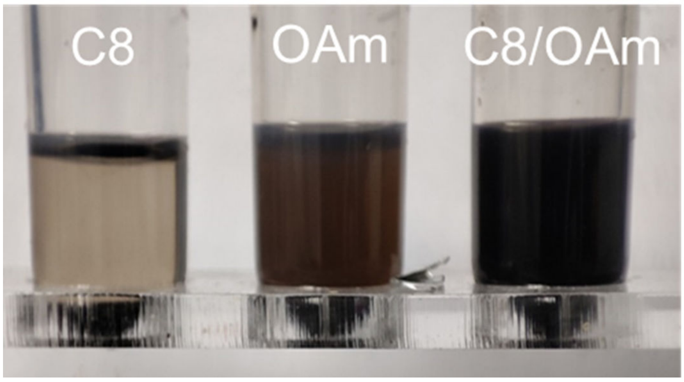

Figure S8. Photographs of varied NiO_x inks after aging for 12 hours. The inks were modulated using C8, OAm, and a combination of C8/OAm with a molar ratio of 4:1.

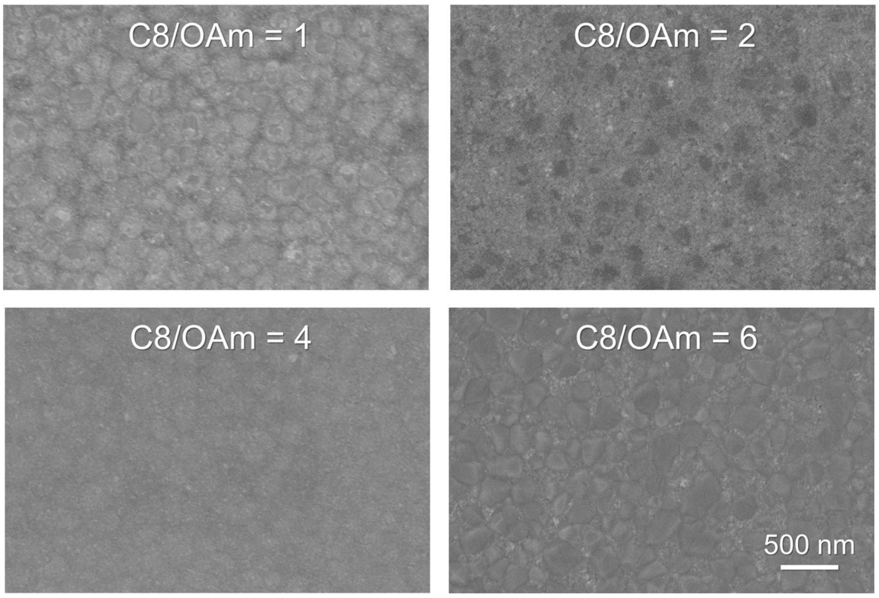

Figure S9. Top-view SEM images of NiO_x films modulated by varied C8/OAm molar ratios.

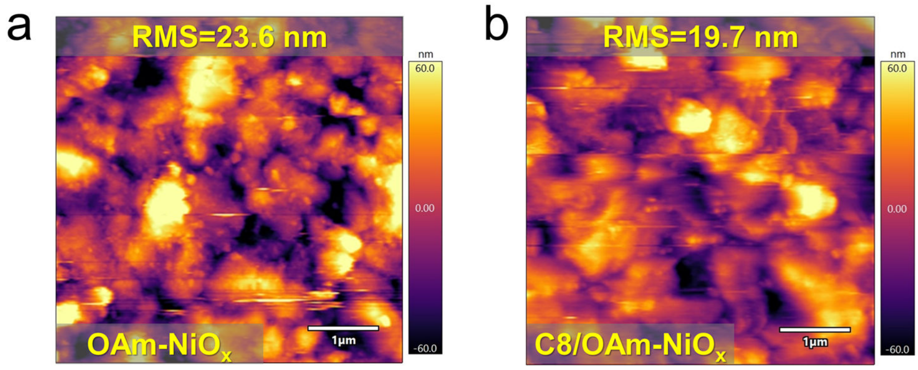

Figure S10. Top-view AFM images of the corresponding FTO/PVK/NiO_x samples.

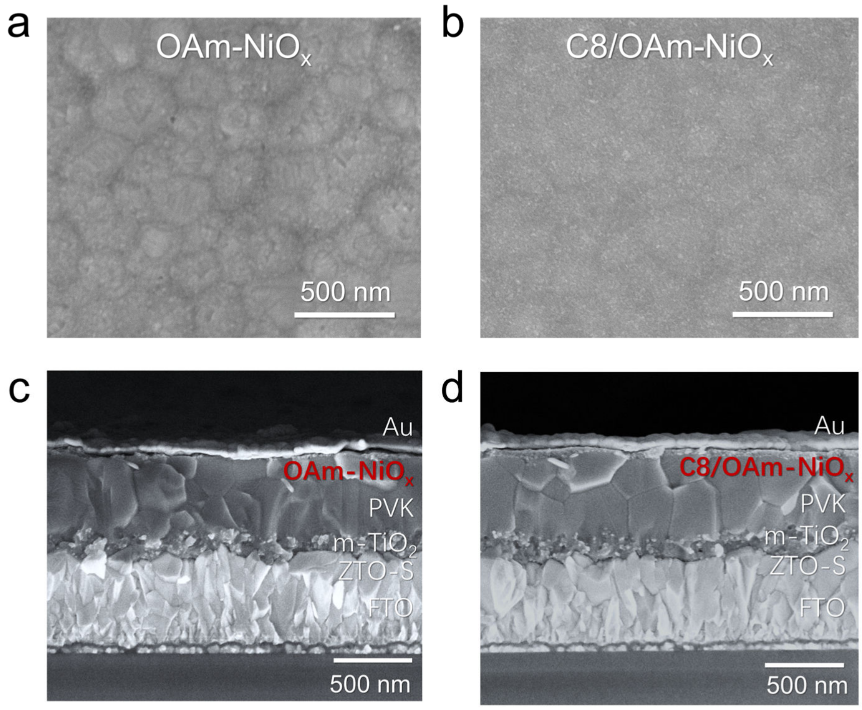

Figure S11. Top-view SEM images of (a) OAm-NiO_x and (b) C8/OAm-NiO_x films on perovskites. Cross-section SEM images of PSCs based on (c) OAm-NiO_x and (d) C8/OAm-NiO_x films.

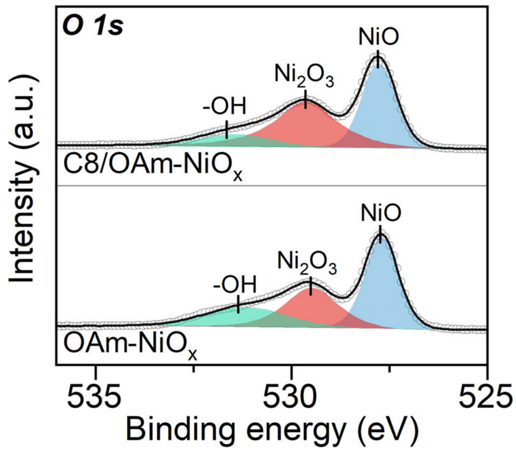

Figure S12. XPS spectra of O 1s core level for the corresponding NiO_x films.

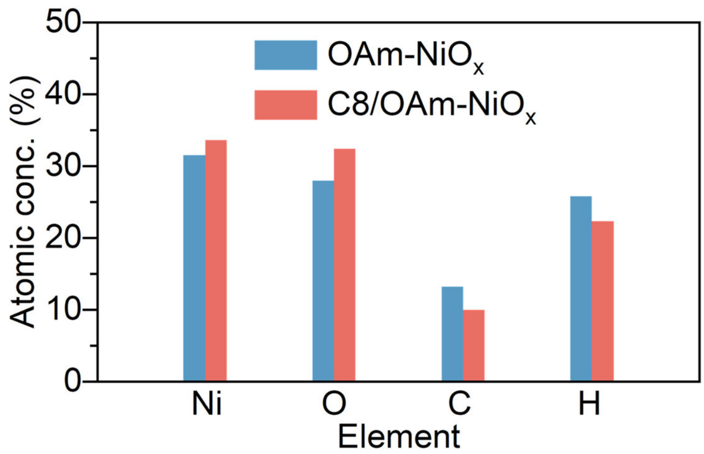

Figure S13. Atomic concentrations of C, Ni, O, and H in the corresponding NiO_x samples.

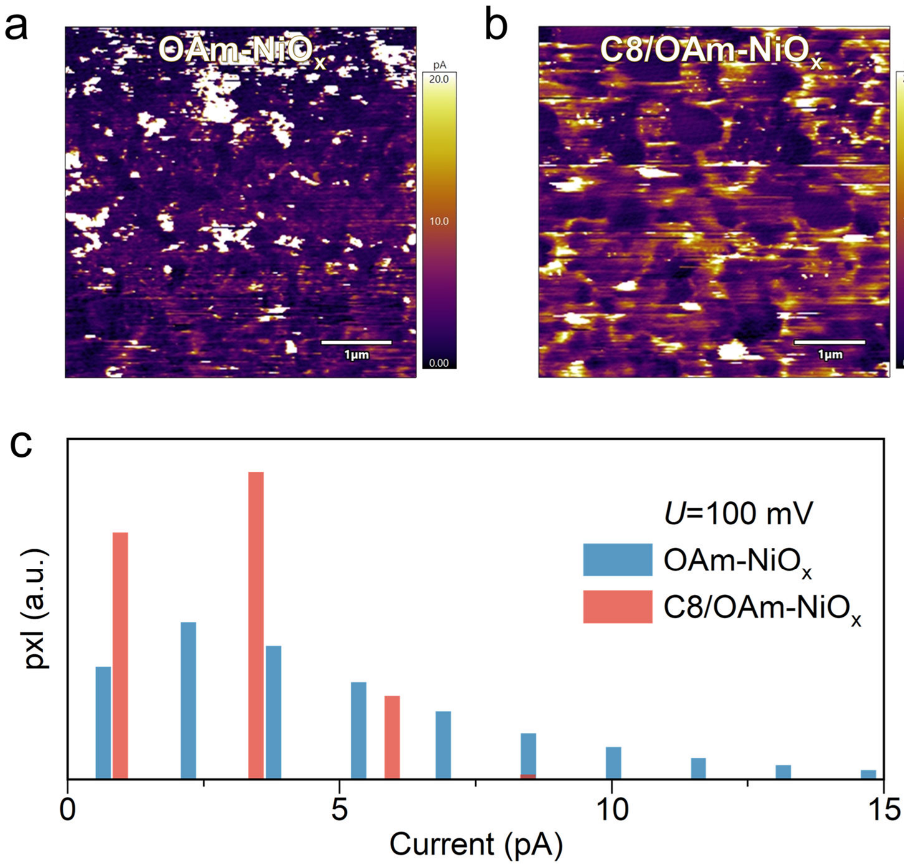

Figure S14. Microscale conductivity of films. (a-b) c-AFM images of the corresponding FTO/PVK/NiO_x samples at a bias potential of 100 mV. (c) Surface current of the films obtained by c-AFM. The C8/OAm-NiO_x film demonstrated a higher and more uniform surface current distribution compared to the OAm-NiO_x film, indicating improved conductivity and uniformity in surface coverage.

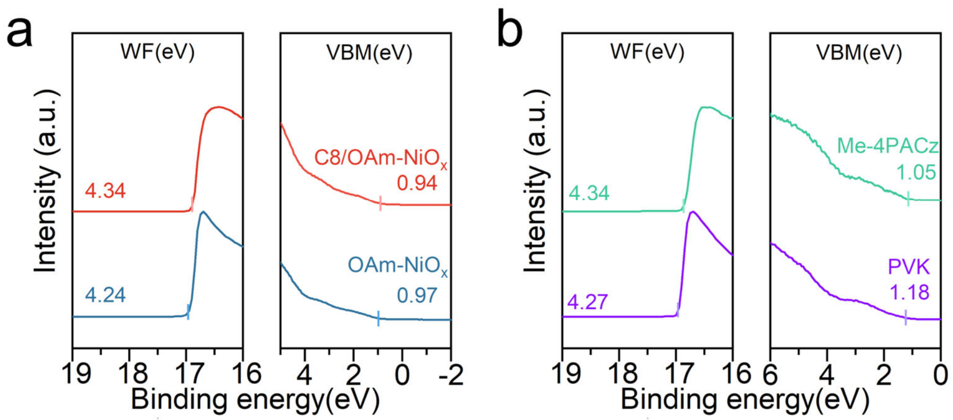

Figure S15. UPS spectra of (a) NiO_x and (b) perovskite films.

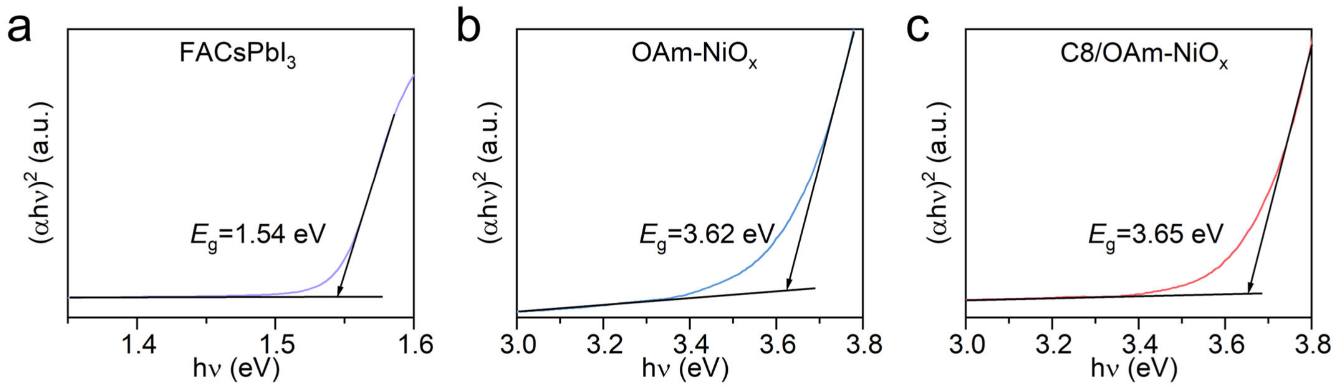

Figure S16. Bandgap measurements. Tauc plots of (a) perovskite, (b) OAm-NiO_x and (c) C8/OAm-NiO_x films.

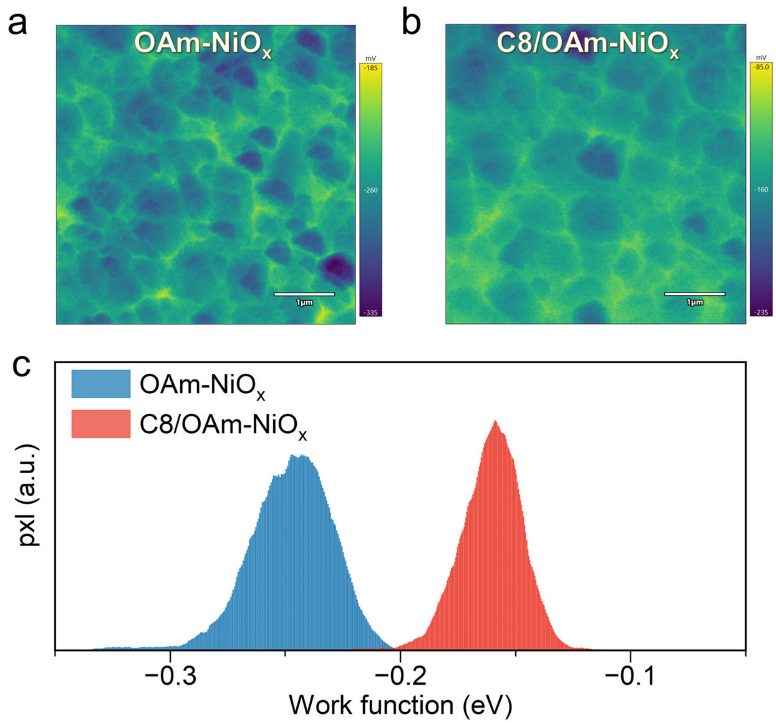

Figure S17. (a-b) KPFM surface potential maps and (c) work function distributions of the corresponding FTO/PVK/NiO_x samples. The mean work function of the C8/OAm-NiO_x film was increased to -0.158 ± 0.037 eV, compared to -0.254 ± 0.046 eV for the OAm-NiO_x film.

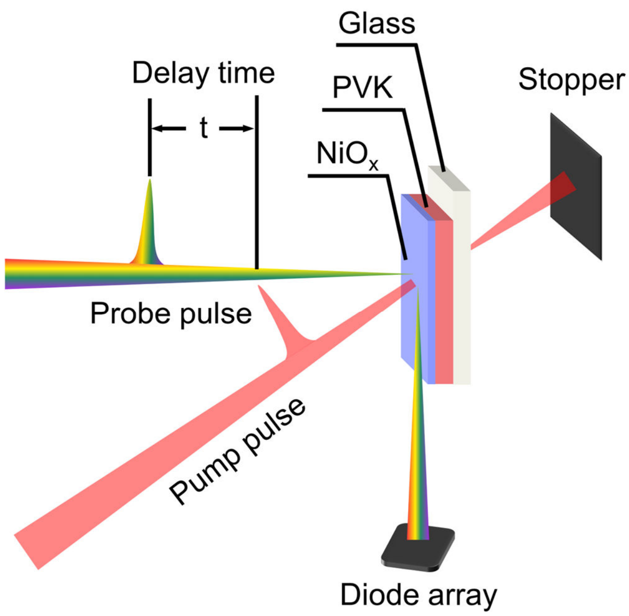

Figure S18. Schematic diagram of the fs-TR measurement for the glass/PVK/NiO_x samples.

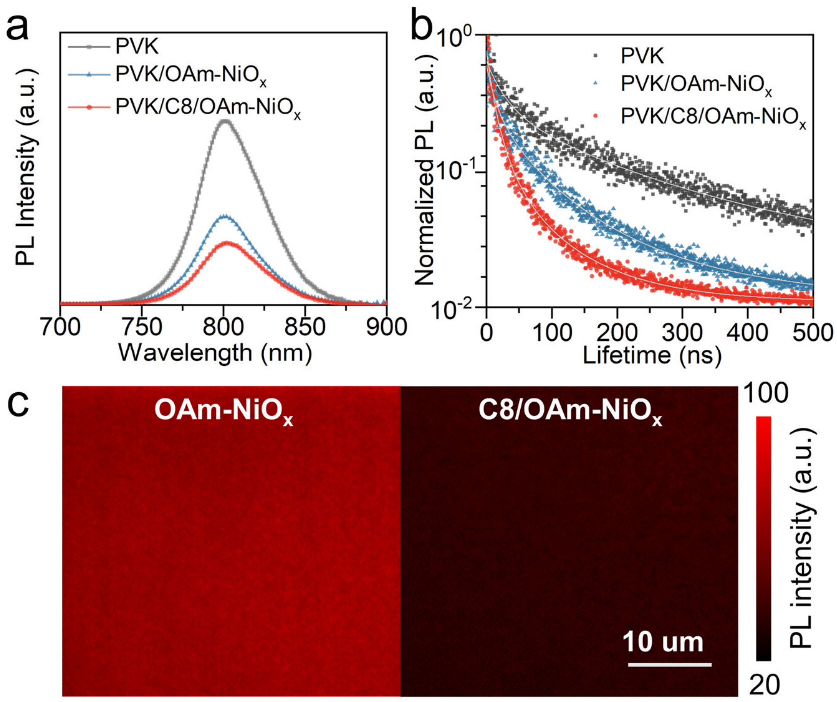

Figure S19. Film quality characterization. (a) Steady-state PL, (b) TRPL and (c) PL mapping spectra of the corresponding films.

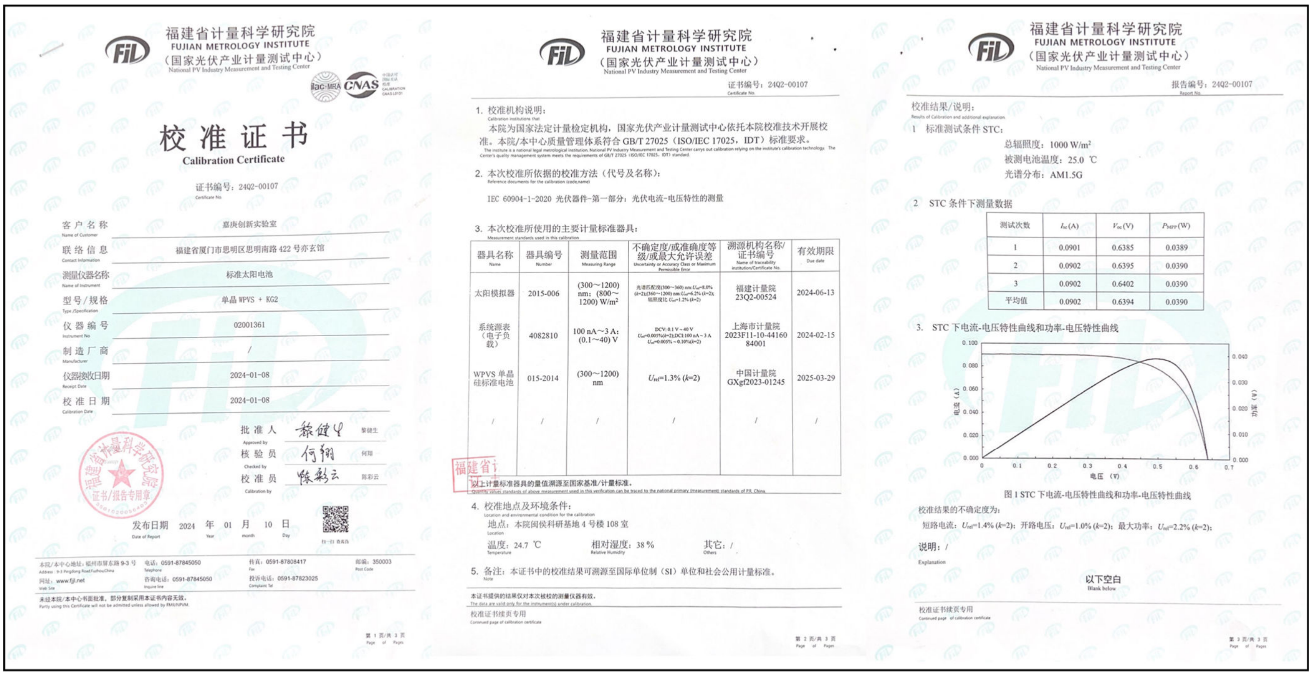

福建省计量科学研究院
FUJIAN METROLOGY INSTITUTE
（国家光伏产业计量测试中心）
National PV Industry Measurement and Testing Center

校 准 证 书
Calibration Certificate

证书编号：24Q2-00107
Certificate No.

客户名称 Name of Customer：嘉庚创新实验室
联络信息 Contact Information：福建省厦门市思明区思明南路 422 号亦玄馆
测量仪器名称 Name of Instrument：标准太阳电池
型号/规格 Type /Specification：单晶 WPVS + KG2
仪器编号 Instrument No：02001361
制造厂商 Manufacturer：/
仪器接收日期 Receipt Date：2024-01-08
校准日期 Calibration Date：2024-01-08

批准人 Approved by：黎健生
核验员 Checked by：何翔
校准员 Calibration by：陈彩云

发布日期 Date of Report：2024 年 01 月 10 日

本院/本中心地址：福州市屏东路 9-3 号 Address：9-3 Pingdong Road,Fuzhou,China
电话：0591-87845050 Telephone
传真：0591-87808417 Fax
邮编：350003 Post Code
网址：www.fjjl.net Web Site
咨询电话：0591-87845050 Inquire line
投诉电话：0591-87823025 Complaint Tel

未经本院/本中心书面批准，部分复制采用本证书内容无效。
Partly using this Certificate will not be admitted unless allowed by FMII/NPVM.

第 1 页/共 3 页

福建省计量科学研究院
FUJIAN METROLOGY INSTITUTE
（国家光伏产业计量测试中心）
National PV Industry Measurement and Testing Center

证书编号：24Q2-00107

1. 校准机构说明：
本院为国家法定计量检定机构，国家光伏产业计量测试中心依托本院校准技术开展校准。本院/本中心质量管理体系符合 GB/T 27025（ISO/IEC 17025，IDT）标准要求。

2. 本次校准所依据的校准方法（代号及名称）：
IEC 60904-1-2020 光伏器件—第一部分：光伏电流-电压特性的测量

3. 本次校准所使用的主要计量标准器具：

器具名称 Name	器具编号 Number	测量范围 Measuring Range	不确定度/或准确度等级/或最大允许误差	溯源机构名称/证书编号	有效期限 Due date
太阳模拟器	2015-006	(300～1200) nm；(800～1200) W/m²	光谱匹配度(300～360) nm: U_{rel}=8.0% (k=2);(360～1200) nm: U_{rel}=6.2% (k=2); 辐照度比 U_{rel}=1.2% (k=2)	福建计量院 23Q2-00524	2024-06-13
系统源表（电子负载）	4082810	100 nA～3 A；(0.1～40) V	DCV: 0.1 V～40 V U_{rel}=0.005%(k=2);DCI:100 nA～3 A U_{rel}=0.005%～0.10%(k=2)	上海市计量院 2023F11-10-4416084001	2024-02-15
WPVS 单晶硅标准电池	015-2014	(300～1200) nm	U_{rel}=1.3% (k=2)	中国计量院 GXgf2023-01245	2025-03-29
/	/	/	/	/	/

以上计量标准器具的量值溯源至国家基准/计量标准。

4. 校准地点及环境条件：
地点：本院闽侯科研基地 4 号楼 108 室
温度：24.7 ℃　相对湿度：38 %　其它：/

5. 备注：本证书中的校准结果可溯源至国际单位制（SI）单位和社会公用计量标准。

本证书提供的结果仅对本次被校的测量仪器有效。
校准证书续页专用

第 2 页/共 3 页

福建省计量科学研究院
FUJIAN METROLOGY INSTITUTE
（国家光伏产业计量测试中心）
National PV Industry Measurement and Testing Center

报告编号：24Q2-00107

校准结果/说明：
1 标准测试条件 STC：
总辐照度：1000 W/m²
被测电池温度：25.0 ℃
光谱分布：AM1.5G

2 STC 条件下测量数据

测试次数	I_{sc} (A)	V_{oc} (V)	P_{MPP} (W)
1	0.0901	0.6385	0.0389
2	0.0902	0.6395	0.0390
3	0.0902	0.6402	0.0390
平均值	0.0902	0.6394	0.0390

3. STC 下电流-电压特性曲线和功率-电压特性曲线

图 1 STC 下电流-电压特性曲线和功率-电压特性曲线

校准结果的不确定度为：
短路电流：U_{rel}=1.4% (k=2)；开路电压：U_{rel}=1.0% (k=2)；最大功率：U_{rel}=2.2% (k=2)；

说明：/

以下空白
Blank below

校准证书续页专用

第 3 页/共 3 页

Figure S20. Calibration certificate for our *J*−*V* test system. To ensure the reliability and credibility of our measurements, we had our *J*−*V* device calibrated by a third-party certification authority. A detailed comparison between our measured open-circuit voltages and current densities and those certified by a third party revealed close agreement, with discrepancies of less than 1.5%. Following this verification, we collected *J*−*V* curves for our devices.

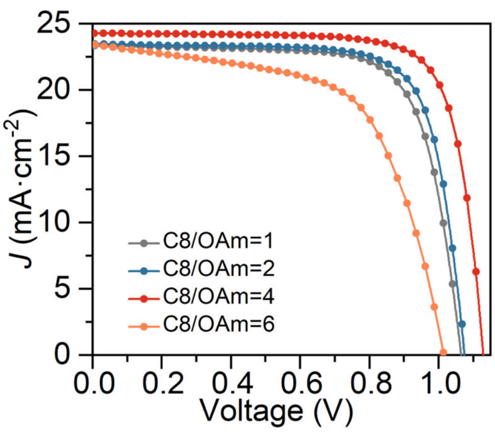

Figure S21. Optimal *J*−*V* curves of PSCs with NiO_x HTLs modulated by C8/OAm at different molar ratios.

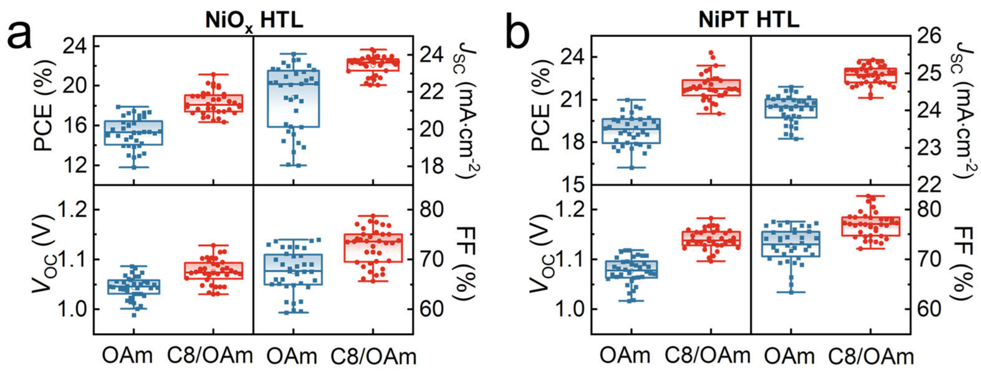

Figure S22. Device performance statistics. Distribution histograms of PCE, J_{SC}, V_{OC} and *FF* for PSCs with (a) NiO_x and (b) NiPT HTLs. Each HTL type comprises 36 cells for statistical analysis and data evaluation. Utilizing the dual ligand strategy, the average PCE of NiO_x-based devices underwent a significant enhancement, rising from 15.28% to 18.30%. Meanwhile, NiPT-based devices also exhibited a notable improvement in their average PCE, increasing from 18.84% to 21.88%.

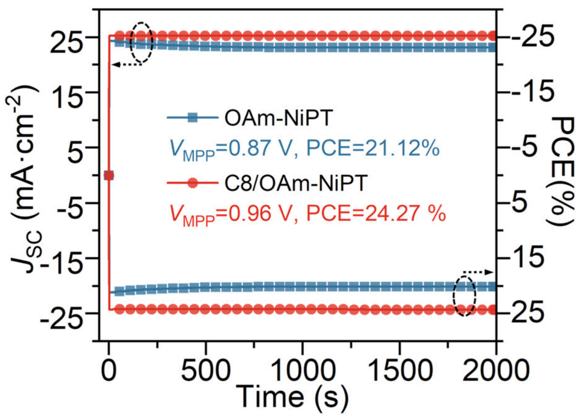

Figure S23. Steady-state power output of unencapsulated PSCs with the corresponding NiP HTLs under maximum power point at atmosphere (~50% RH).

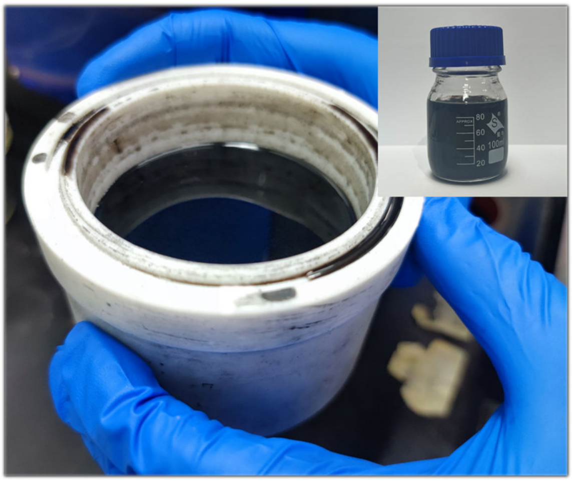

Figure S24. Scale-up production of the NiO_x ink via a ball-milling method.

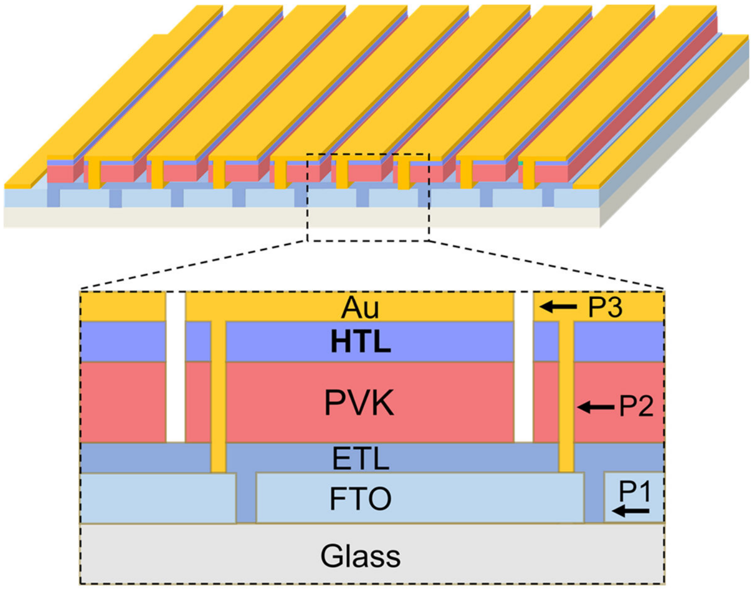

Figure S25. Structural schematic diagram of 6×6 cm^2 PSM.

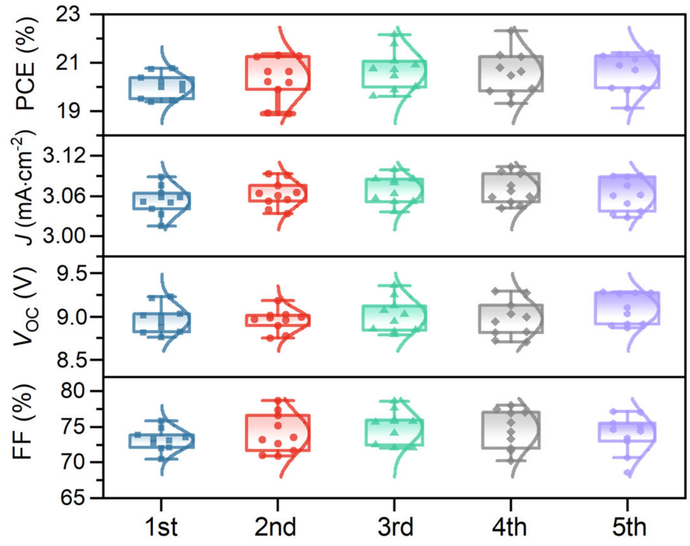

Figure S26. Statistical distribution of 50 PSMs incorporating C8/OAm-NiPT HTLs, sourced from five distinct synthesis batches. Each PSM boasts an active area of 21.8 cm², achieving a champion PCE of 22.34% and an average PCE of 20.44%.

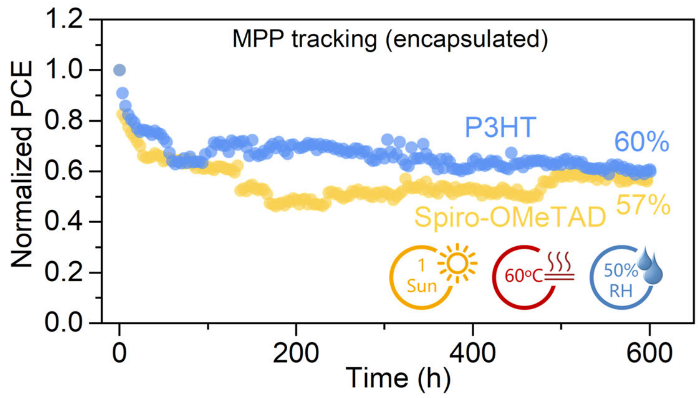

Figure S27. MPP tracking of encapsulated modules employing P3HT and spiro-OMeTAD as HTLs under simulated one-sun illumination, 60°C and 50% RH.

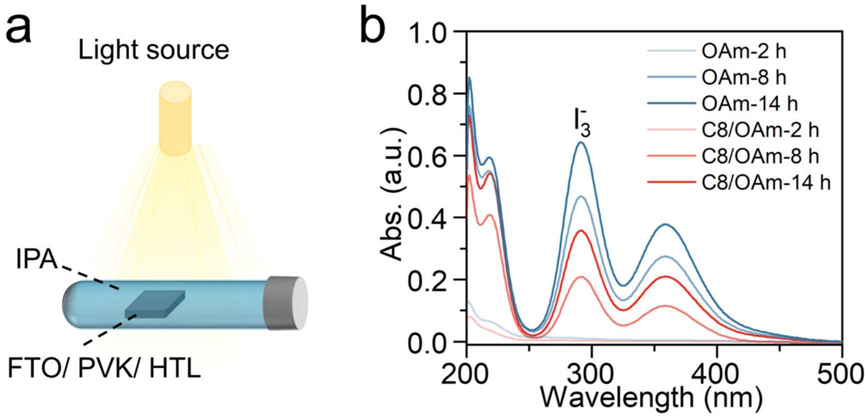

Figure S28. Iodine-escape analysis in perovskite films with the corresponding HTLs. (a) Schematic of the experimental setup designed for real-time monitoring of iodine migration from perovskite films. (b) UV-vis absorption spectra of the IPA solvent recorded during the aging process. In this experiment, perovskite films coated with varied HTLs were fully immersed in IPA within a nitrogen-sealed vial and exposed to full-spectrum sunlight under ambient conditions. This setup enables a precise assessment of iodine loss from the films. Rapid extraction of I_3^- ions indicates active iodine migration upon illumination.[S1] However, the C8/OAm-NiPT HTLs reduces iodine migration, which is beneficial to operational stability.

Table S1. Photovoltaic parameters of the corresponding devices with NiO_x HTLs modulated by OAm at different molar ratios.

Entry	V_{OC} **(V)**	J_{SC} **(mA cm^{-2})**	***FF*** **(%)**	**PCE (%)**
OAm/NiO_x-0.3%	0.912	22.36	47.78	9.74
OAm/NiO_x-1.5%	0.958	23.11	60.34	13.36
OAm/NiO_x-3.0%	1.046	23.20	73.65	17.87
OAm/NiO_x-4.5%	1.052	18.79	64.82	12.81
OAm/NiO_x-6.0%	0.820	17.71	53.15	7.72

Table S2. Element analysis of the corresponding NiO_x sample. The estimation of Ni content is determined by subtracting the combined content of C, H, N, and O.

Entry	C (wt%)	H (wt%)	N (wt%)	O (wt%)	Ni (wt%)	C/Ni (mol%)
OAm-NiO_x-1	6.47	1.06	0.85	18.15		
OAm-NiO_x-2	6.29	1.01	0.82	17.69		
Ave.	**6.38**	**1.03**	**0.84**	**17.92**	**73.83**	**42.1**
C8/OAm-NiO_x-1	4.74	0.88	0.87	19.34		
C8/OAm-NiO_x-2	4.30	0.80	0.88	19.38		
Ave.	**4.52**	**0.84**	**0.88**	**19.51**	**74.25**	**29.7**

Table S3. Hall effect measurements of the corresponding NiO_x films.

Entry	Type	Hall coefficient (cm^3 C^{-1})	Carrier concentration (cm^{-3})
OAm-NiO_x	p	3.01±0.37	$(2.25\pm0.25)\times10^{18}$
C8/OAm-NiO_x	p	0.85±0.16	$(9.06\pm1.65)\times10^{18}$

Table S4. TRPL decay curves lifetime fitting of PVK and PVK-NiO_x films. TRPL curves were fitted using a bi-exponential decay equation of $I(t) = I_0 + A_1\exp(-t/\tau_1) + A_2\exp(-t/\tau_2)$.

Entry	A_1 (%)	τ_1 (ns)	A_2 (%)	τ_2 (ns)
PVK	16.19	32.81	63.44	470.39
PVK/OAm-NiO_x	14.45	16.34	70.45	192.27
PVK/C8/OAm-NiO_x	30.51	22.65	60.59	118.57

Table S5. Photovoltaic parameters of the corresponding devices with NiO_x HTLs modulated by C8/OAm at different molar ratios.

Entry	V_{OC} (V)	J_{SC} (mA cm^{-2})	*FF* (%)	PCE (%)
C8/OAm=1	1.064	23.33	73.30	18.19
C8/OAm=2	1.073	23.45	75.47	18.99
C8/OAm=4	1.128	24.27	77.10	21.12
C8/OAm=6	1.013	23.40	61.16	14.50

Table S6. Photovoltaic parameters of the corresponding devices with NiO_x HTLs.

Entry	Scan direction	V_{OC} (V)	J_{SC} (mA cm^{-2})	*FF* (%)	PCE (%)
OAm-NiO_x	Reverse	1.046	23.20	73.65	17.87
	Forward	1.015	22.80	62.63	14.51
C8/OAm-NiO_x	Reverse	1.128	24.27	77.10	21.12
	Forward	1.097	24.15	74.80	19.82

Table S7. Photovoltaic parameters of the corresponding devices with NiPT HTLs.

Entry	Scan direction	V_{OC} (V)	J_{SC} (mA cm^{-2})	*FF* (%)	PCE (%)
OAm-NiPT	Reverse	1.118	24.25	77.40	20.99
	Forward	1.092	24.20	70.21	18.55
C8/OAm- NiPT	Reverse	1.168	25.35	82.10	24.32
	Forward	1.145	25.25	77.43	22.39

Table S8. Fitted data of charge transport resistance (R_{tr}) and charge recombination resistance (R_{rec}) of devices utilizing NiO_x HTLs.

Entry	R_{tr} (kΩ)	R_{rec} (kΩ)
OAm-NiPT	9.46	86.65
C8/OAm- NiPT	5.23	103.11

Table S9. Total material cost for the amine-modulated NiPT ink encompasses the expenses incurred for raw materials and solvent. The data were sourced from the online website: https://www.inno-chem.com.cn.

Raw material	Brand	Retail price *US $* (quantity)	Experimental dosage	Experimental consumption *US$*	Yield
P3HT	Innochem	198 (1 g)	0.55 g	109	367.7 mL (84%)
$Ni(NO_3)_2{\cdot}6H_2O$	Sinopharm	25 (500 g)	58 g	2.900	
NaOH	Sinopharm	3.5 (500 g)	1.2 g	0.084	
C8	Sigma-aldrich	121 (1 L)	1.11 mL	0.135	
OAm	Sigma-aldrich	197 (500 g)	0.44 g	0.173	
CB	Alfa Aesar	83 (1 L)	367.7 mL	30.5	
NiPT	Lab-synthesized			142.8	0.39 *US$* mL^{-1}

Table S10. Total materials cost for the Spiro-OMeTAD solution[S2] encompasses the expenses incurred for raw materials and solvent.

Raw material	**Brand**	**Retail price *US $* (quantity)**	**Experimental dosage**	**Experimental consumption *US$***	**Yield**
Spiro-OMeTAD	TCI	174 (1 g)	9.4 g	1635.6	107.1 mL
Li-TFSI	Sigma-aldrich	85 (5 g)	1.2 g	20.4	
Co-TFSI	Sigma-aldrich	127 (5 g)	0.34 g	8.64	
*t*BP	Alfa Aesar	145 (1 L)	3.9 mL	0.57	
acetonitrile	Alfa Aesar	92 (1 L)	3.2 mL	0.3	
CB	Alfa Aesar	83 (1 L)	100 mL	8.3	
Spiro-OMeTAD solution	Lab-prepared			1673.80	15.63 *US$* mL^{-1}

Table S11. Total materials cost for the PTAA solution[S3] encompasses the expenses incurred for raw materials and solvent.

Raw material	**Brand**	**Retail price *US $* (quantity)**	**Experimental dosage**	**Experimental consumption *US$***	**Yield**
PTAA	TCI	974 (1 g)	1.5 g	1461	101.75 mL
Li-TFSI	Sigma-aldrich	85 (5 g)	0.135 g	2.3	
*t*BP	Alfa Aesar	145 (1 L)	1 mL	0.15	
acetonitrile	Alfa Aesar	92 (1 L)	0.75 mL	0.12	
CB	Alfa Aesar	83 (1 L)	100 mL	8.3	
PTAA solution	Lab-prepared			1471.87	14.47 *US$* mL^{-1}

Table S12. Summary of efficiency and stability of NiO_x-based mini-modules from publicly reported data. IE: Initial efficiency.

n-i-p structure

Device structure	Highlight	Efficiency	Module stability	Ref.
FTO/ZTO/CsFAMAPb(IBr)$_3$/ NiO_x-P3HT/Au	Organic inorganic hybrid HTL	16.8% (18 cm^2)	91% IE (85°C/85% RH for 1000 h); 80% IE (MPP tracking at 85°C for 166 h)	S4
FTO/ZTO/FAMAPb(IBr)$_3$/ QDs/NiO_x/Au	Inorganic QDs passivation	19.1% (18 cm^2)	91% IE (85°C/85% RH for 1000 h); 90% IE (MPP tracking at 50°C for 16 h)	S5
FTO/ZTO/CsFAMAPb(IBr)$_3$/ NiO_x-P3HT/Au	NiO_x passivator; Multi-defect management	17.0% (18 cm^2)	87% IE (85°C/85% RH for 2000 h); 100% IE (MPP tracking at 60°C for 1600 h)	S6
FTO/ZTO/CsFAPbI$_3$/Me-4PACz/NiO_x-P3HT/Au	Ligand engineering	22.3% (21.8 cm^2)	99% IE (85°C for 500 h); 95% IE (MPP tracking at 60°C for 700 h)	This work

p-i-n structure

Device structure	Highlight	Efficiency	Module stability	Ref.
FTO/NiO_x/Me-4PACz/ $FAPbI_3$/PCBM/SnO_2/Cu	H_2O_2 for homogeneous nickel oxide	21.0% (14.7 cm^2)	n/a	S7
FTO/NiO_x/urea/CsFAMA Pb(IBr)$_3$/C_{60}/BCP/Ag	Urea passivation	19.0% (16 cm^2) 17.2% (196 cm^2)	n/a	S8

ITO/NiO_x/PTAA/CsFAMAPb $(IBr)_3$/PCBM/BCP/Ag	2D/3D perovskite	21.6% (19.3 cm^2)	n/a	S9
ITO/NiO_x/2PACz/ $FAPbI_3$/C_{60}/BCP/Au	Vacuum-assisted growth	18.3% (12.3 cm^2)	100% IE (MPP tracking at 85°C for 20 h)	S10
ITO/NiO_x/CsFAMAPb$(IBr)_3$/ LiF_x/C_{60}/BCP/Cu	Co-evaporation of PbI_2/CsBr layer	19.8% (16 cm^2)	n/a	S11
ITO/NiO_x/MeO-2PACz/ $FACsPbI_3$/ C_{60}/BCP/Cu	THF co-solvent dilution	12.6% (110 cm^2)	84 % IE (MPP tracking at 85°C for 1000 h)	S12
FTO/NiO_x/LiF/CsFAMAPb $(IBr)_3$/C_{60}/BCP/Cu	LiF evaporation for NiO_x doping	19.5% (57.3 cm^2)	80% IE (MPP tracking for 700 h)	S13
FTO/NiO_x/NCS/ CsFAMAPb$(IBr)_3$/ PCBM/BCP/Ag	NCS passivation	21.2% (18 cm^2)	n/a	S14
ITO/NiO_x/ MeO-2PACz/ $MAPbI_3$/ PCBM/BCP/Cu	CBD NiO_x	19.0% (18.1 cm^2)	n/a	S15
FTO/NiO_x/KBH_4/CsFAMA PbI_3/ PCBM/BCP/Ag	KBH_4 for synergistic redox modulation	20.2% (29 cm^2)	94% IE (MPP tracking at 65°C for 2000 h)	S16
ITO/NiO_x/ NA-Me/FACs PbI_3/PCBM/BCP/Ag	Buried interface molecular hybrid	22.7% (11.1 cm^2)	n/a	S17
FTO/NiO_x/$CsFAPbI_3$/ PCBM/BCP/Ag	Surface redox engineering	18.6% (174 cm^2)	80% IE (aging in ambient environment for 1500 h)	S18
ITO/NiO_x/ CsFAPb$(IBr)_3$/ PEABr/PMMA/C_{60}/BCP/Ag	Modulation of A-site cations eliminates DMSO adsorption	19.1% (18 cm^2)	84% IE (MPP tracking for 1056 h)	S19
FTO/NiO_x/FAMAPb$(IBr)_3$/PM MA/PCBM/BCP/Ag	Flash infrared annealing for NiO_x	16.7% (17 cm^2)	n/a	S20

Table S13. Summary of NiO_x-based HTLs in n-i-p PSCs.

Device structure	V_{OC} [V] (C/T)	J_{SC} [mA cm^{-2}] (C/T)	*FF* [%] (C/T)	PCE [%] (C/T)	Year	Ref.
FTO/TiO_2/$MAPbI_3$/NiO_x/Au	0.38 0.88	15.75 19.49	30.8 53.1	1.8 9.1	2017	S21
FTO/TiO_2/$MAPbI_3$/NiO_x/ MWCNT	0.90 0.91	21.03 22.84	74.4 76.0	14.1 15.8	2017	S22
FTO/TiO_2/$MAPbI_3$/NiO_x/Au	0.83 0.97	15.03 18.12	52.0 62.0	6.5 10.9	2018	S23
FTO/TiO_2/$CsPbI_2Br$/ NiO_x/Au	1.07 1.26	14.51 15.12	51.5 79.8	8.9 15.1	2019	S24
FTO/TiO_2/CsFAMAPb(IBr)$_3$ /NiO_x/Au	0.80 0.99	18.10 21.90	38.0 60.0	5.5 13.1	2019	S25
FTO/SnO_2/CsFAMAPb(IBr)$_3$ /NiO_x/Au	0.69 1.04	21.16 22.53	39.2 54.4	5.8 12.7	2019	S26
FTO/TiO_2/CsFAMAPb(IBr)$_3$ /Cs:NiO_x/CuSCN/Au	1.03 1.10	22.10 23.15	73.6 75.7	17.2 19.2	2019	S27
ITO/SnO_2/FAMAPbI(IBr)$_3$ /NiO_x/Spiro-OMeTAD/Au	1.10 1.14	23.03 23.82	78.2 79.8	19.8 21.6	2019	S28
FTO/TiO_2/CsFAPb(IBr)$_3$ /NiO_x/CNT/Carbon	0.89 0.97	16.55 18.30	54.0 64.0	7.9 11.4	2021	S29
FTO/SnO_2/FAMAPb(IBr)$_3$ /NiO_x/Au	1.07 1.07	24.08 24.96	65.7 71.3	16.9 19.1	2021	S30
FTO/SnO_2/FAMAPb(IBr)$_3$ /NiO_x/ITO	1.08 1.08	23.27 23.33	71.7 77.3	18.0 19.5	2022	S31
FTO/ZTO/CsFAMAPb(IBr)$_3$ /NiO_x-P3HT/Au	1.02 1.15	23.37 24.07	66.8 76.5	16.0 21.2	2022	S4
FTO/ZTO/FAMAPb(IBr)$_3$ /QDs/NiO_x/Au	1.08 1.11	23.62 24.86	73.3 78.1	18.8 21.9	2022	S5
ITO/SnO_2/$FAPbI_3$/PDCBT /NiO_x /Au	1.09 1.18	25.20 25.30	78.9 79.8	21.7 23.8	2024	S32
ITO/SnO_2/CsFAMAPb(IBr)$_3$ /NiO_x-F4TCNQ/Ag	1.18 1.20	25.36 25.24	78.2 83.3	23.3 25.2	2024	S33
FTO/ZTO/$CsFAPbI_3$ /Me-4PACz/NiO_x-P3HT/Au	1.12 1.17	24.25 25.35	77.4 82.1	21.0 24.3	2025	This work

Supplemental References:

S1. G. Y. Kim, A. Senocrate, T. Y. Yang, G. Gregori, M. Gratzel and J. Maier, *Nat. Mater.*, 2018, **17**, 445-449.

S2. M. J. Paik, Y. Y. Kim, J. Kim, J. Park and S. I. Seok, *Joule*, 2024, **8**, 2073-2086.

S3. Z. Huang, Y. Bai, X. Huang, J. Li, Y. Wu, Y. Chen, K. Li, X. Niu, N. Li, G. Liu, Y. Zhang, H. Zai, Q. Chen, T. Lei, L. Wang and H. Zhou, *Nature*, 2023, **623**, 531-537.

S4. F. Cao, F. Cheng, X. Huang, X. Dai, Z. Tang, S. Nie, J. Yin, J. Li, N. Zheng and B. Wu, *Adv. Funct. Mater.*, 2022, **32**, e2201423.

S5. F. Cheng, F. Cao, B. Chen, X. Dai, Z. Tang, Y. Sun, J. Yin, J. Li, N. Zheng and B. Wu, *Adv. Sci.*, 2022, **9**, e2201573.

S6. F. Cao, S. Q. Zhan, X. F. Dai, F. W. Cheng, W. X. Li, Q. F. Feng, X. F. Huang, J. Yin, J. Li, N. F. Zheng and B. H. Wu, *J. Am. Chem. Soc.*, 2024, **146**, 11782-11791.

S7. S. Yu, Z. Xiong, H. Zhou, Q. Zhang, Z. Wang, F. Ma, Z. Qu, Y. Zhao, X. Chu, X. Zhang and J. You, *Science*, 2023, **382**, 1399-1404.

S8. C. Li, Y. Zhang, X. Zhang, P. Zhang, X. Yang and H. Chen, *Adv. Funct. Mater.*, 2023, **33**, 2214774.

S9. Y. Huang, K. Yan, B. Niu, Z. Chen, E. Gu, H. Liu, B. Yan, J. Yao, H. Zhu, H. Chen and C.-Z. Li, *Energy Environ. Sci.*, 2023, **16**, 557-564.

S10. H. Hu, D. B. Ritzer, A. Diercks, Y. Li, R. Singh, P. Fassl, Q. Jin, F. Schackmar, U. W. Paetzold and B. A. Nejand, *Joule*, 2023, **7**, 1574-1592.

S11. A. Z. Afshord, B. E. Uzuner, W. Soltanpoor, S. H. Sedani, T. Aernouts, G. Gunbas, Y. Kuang and S. Yerci, *Adv. Funct. Mater.*, 2023, **33**, e2301695.

S12. F. Jafarzadeh, L. A. Castriotta, E. Calabrò, P. Spinelli, A. Generosi, B. Paci, D. Becerril Rodriguez, M. Luce, A. Cricenti, F. Di Giacomo, F. Matteocci, F. Brunetti and A. Di Carlo, *Commun. Mater.*, 2024, **5**, 186.

S13. L. Wang, X. Li, S. Yuan, F. Qian, Z. Kang and S. Li, *Symmetry*, 2024, **16**, 1357.

S14. Y. Yang, R. Chen, J. Wu, Z. Dai, C. Luo, Z. Fang, S. Wan, L. Chao, Z. Liu and H. Wang, *Angew. Chem. Int. Ed.*, 2024, **63**, e202409689.

S15. S. Li, X. Wang, H. Li, J. Fang, D. Wang, G. Xie, D. Lin, S. He and L. Qiu, *Small*, 2023, **19**, e2301110.

S16. Y. Liu, B. Ding, G. Zhang, X. Ma, Y. Wang, X. Zhang, L. Zeng, M. K. Nazeeruddin, G. Yang and B. Chen, *Adv. Sci.*, 2024, **11**, e2309111.

S17. S. Liu, J. Li, W. Xiao, R. Chen, Z. Sun, Y. Zhang, X. Lei, S. Hu, M. Kober-Czerny, J. Wang, F. Ren, Q. Zhou, H. Raza, Y. Gao, Y. Ji, S. Li, H. Li, L. Qiu, W. Huang, Y. Zhao, B. Xu, Z. Liu, H. J. Snaith, N.-G. Park and W. Chen, *Nature*, 2024, **632**, 536-542.

S18. M. Du, S. Zhao, L. Duan, Y. Cao, H. Wang, Y. Sun, L. Wang, X. Zhu, J. Feng, L. Liu, X. Jiang, Q. Dong, Y. Shi, K. Wang and S. Liu, *Joule*, 2022, **6**, 1931-1943.

S19. S. Li, X. Wang, J. Fang, D. Lin, N. Huang, D. Wang, S. He and L. Qiu, *Chem. Eng. J.*, 2024, **490**, 151919.

S20. E. Ochoa-Martinez, S. Bijani-Chiquero, M. d. V. Martínez de Yuso, S. Sarkar, H. Diaz-Perez, R. Mejia-Castellanos, F. Eickemeyer, M. Grätzel, U. Steiner and J. V. Milić, *Adv. Sci.*, 2023, **10**, 2302549.

S21. Z. Liu, A. Zhu, F. Cai, L. Tao, Y. Zhou, Z. Zhao, Q. Chen, Y.-B. Cheng and H. Zhou, *J. Mater. Chem. A*, 2017, **5**, 6597-6605.

S22. Y. L. Yang, H. N. Chen, X. L. Zheng, X. Y. Meng, T. Zhang, C. Hu, Y. Bai, S. Xiao and S. H. Yang, *Nano Energy*, 2017, **42**, 322-333.

S23. K. C. Icli and M. Ozenbas, *Electrochim Acta*, 2018, **263**, 338-345.

S24. W. T. Chen, S. S. Zhang, Z. H. Liu, S. H. Wu, R. Chen, M. Pan, Z. C. Yang, H. M. Zhu, S. W. Liu, J. Tang, J. Y. Li and W. Chen, *Sol. RRL*, 2019, **3**, 1900346.

S25. R. Kaneko, H. Kanda, K. Sugawa, J. Otsuki, A. Islam and M. K. Nazeeruddin, *Sol. RRL* 2019, **3**, 1900172.

S26. J. Tirado, M. Vásquez-Montoya, C. Roldán-Carmona, M. Ralaiarisoa, N. Koch, M. K. Nazeeruddin and F. Jaramillo, *ACS Appl. Energy Mater.*, 2019, **2**, 4890-4899.

S27. S. S. Mali, J. V. Patil, H. Kim, R. Luque and C. K. Hong, *Mater. Today*, 2019, **26**, 8-18.

S28. R. Li, P. Wang, B. Chen, X. Cui, Y. Ding, Y. Li, D. Zhang, Y. Zhao and X. Zhang, *ACS Energy Lett.*, 2019, **5**, 79-86.

S29. P. Kartikay, D. Sadhukhan, A. Yella and S. Mallick, *Sol. Energy Mater. Sol. Cells*, 2021, **230**, 111241.

S30. S. Y. Park, S. J. Kim, J. H. Lee, M. J. Jeong, J. M. Lee, H. S. Jung and J. H. Noh, *Adv. Funct. Mater.*, 2021, **31**, 2100863.

S31. M. J. Jeong, J. H. Lee, C. H. You, S. Y. Kim, S. Lee and J. H. Noh, *Adv. Energy Mater.*, 2022, **12**, 2200661.

S32. H. Liu, Y. Gao, F. Xu, X. Zhang, A. Ullah, L. Xu, S. Zhang, J. Wang, S. De Wolf and H. L. Wang, *Adv. Funct. Mater.*, 2024, **34**, 2315843.

S33. Y. Xu, Z. Chu, H. Wang, Z. Xing, B. Fan, X. Hu and Y. Chen, *Sci. China Chem.*, 2024, **67**, 2335-2340.